Chemical independent relaxation in metallic glasses from the nanoindentation experiments

S. Ouyang,[1] L. S. Huo,[1] Y. Yang,[2,a)] W. Xu,[1] J. T. Huo,[1] J. Q. Wang,[1,a)] X. M. Wang,[1] and R. W. Li[1]

[1]*CAS Key Laboratory of Magnetic Materials and Devices and Zhejiang Province Key Laboratory of Magnetic Materials and Application Technology, Ningbo Institute of Materials Technology and Engineering, Chinese Academy of Sciences, Ningbo, Zhejiang 315201, China*

[2]*Centre for Advanced Structural Materials, Department of Mechanical and Biomedical Engineering, City University of Hong Kong, Tat Chee Avenue, Kowloon Tong, Kowloon, Hong Kong, China*

(Received 21 March 2017; accepted 11 June 2017; published online 26 June 2017)

In this article, we studied the anelastic properties at low-load nanoindentations of different metallic glasses, including Zr-, Pd-, La-, Mg-, and Au-bases. It is verified that the "two-parameter Kelvin model" is suitable for analyzing the anelastic mechanical behavior. Despite the difference in the chemical composition of these alloys, the energy barrier against the local relaxation is almost equal. The energy barrier is much smaller than that of slow β relaxation, which denotes a faster relaxation mechanism. These findings give insights into the heterogeneous nature of mechanical behavior and relaxation characteristics of metallic glasses. *Published by AIP Publishing.*
[http://dx.doi.org/10.1063/1.4989825]

I. INTRODUCTION

Metallic glasses (MGs) are well known to exhibit outstanding physical or chemical properties, such as high strength and hardness, excellent corrosion resistance, and soft magnetic properties.[1] These advanced properties make them promising candidates as materials with structural and functional properties. When MGs are quenched from liquids through glass transition, they inherit the disordered structure of liquids with a large number of quenched-in defects.[2–7] Recently, a series of findings have suggested the existence of structural heterogeneity in metallic glasses at the nanometer scale.[6,8] The loose atomic packing regions such as the "structural defects" are embedded in the elastic matrix.[9,10] The mechanical properties can be obviously regulated by the structural heterogeneities.[9–11]

Plentiful research efforts have been devoted to revealing the disordered structure in MGs[7,12–14] and to exploring the correlation between the microstructure and macro-mechanical properties.[14–17] Simulations have advanced in characterizing the atomic packing structures. However, for liquid-like zones or flow units that have a larger size, simulations do not work. Recent experiments reveal that there is probably a universal nanoscale heterogeneity in metallic glasses that is akin to liquid-like zones.[9,10,18,19] Studying the kinetics of liquid-like zones and their evolution is helpful for understanding their influences on macro-mechanical properties.

The plastic deformation of MGs is determined by the formation and propagation of shear bands.[20,21] It is proposed that shear bands derive from the nucleation and percolation of shear transformation zones that is akin to liquid-like zones.[15,22] Given the small size of shear band and shear transformation zones, nanoindentation is a powerful method for experimentally studying their kinetics.[20,23–26] The MGs deform elastically and the load-displacement curve can be fitted very well using the Hertzian elastic contact theory at a suitable loading rate.[27] Shear band nucleation can be detected if the load is high enough where pop-in events occur.[24,26]

Especially, the anelastic behavior that reveals the mechanical heterogeneity of MGs can be detected at fast loading-unloading rates.[28] For fitting the dynamic anelastic behavior, a Kelvin model with two parameters and a developed three-parameter model are proposed. The Kelvin viscoelastic model[28,29] contains a dash pot and a spring in parallel, while another spring is added in series to the dash pot for the three-parameter model.[30,31] The three-parameter viscoelastic model has shown that the shear modulus of MGs can be determined by two concurrent contributions of the elastic matrix and liquid-like zones in the nanoindentation experiment.[30,31] These two models are proper to study the rheological properties and relaxation dynamics in amorphous materials.

In this work, we studied the anelastic behaviors of five metallic glasses with different compositions and macro properties using low-load nanoindentation. The Kelvin model can give a better interpretation for the detected anelastic behavior rather than the three-parameter model. It is found that the activation energy for structural evolution is very small compared to slow-β relaxation and is almost a constant that is independent of the chemical compositions of metallic glasses.

II. EXPERIMENTAL DETAILS

In the present work, we use five MGs with nominal compositions of $Zr_{52.5}Ti_5Cu_{17.9}Ni_{14.6}Al_{10}$ (Vit105), $Pd_{40}Ni_{10}Cu_{30}P_{20}$, $La_{60}Ni_{15}Al_{25}$, $Mg_{61}Cu_{28}Gd_{11}$, and $Au_{60}Cu_{15.5}Ag_{7.5}Si_{17}$ as model materials to study the kinetics of liquid-like

a)Authors to whom correspondence should be addressed: yonyang@cityu.edu.hk and jqwang@nimte.ac.cn

TABLE I. The calculated parameters in the Kelvin anelastic model for different MGs at low indentation loads. Here kT is used as the unit of ΔE. The data of Vit105 is from Ref. 30.

Materials	Load (μN)	G_K (GPa)	η (MPa s)	t_c (ms)	ΔE (kT)
Vit105	400	33.4 ± 2.4	9.07 ± 1.40	0.32 ± 0.07	22.6 ± 0.3
	600	34.1 ± 1.2	9.18 ± 1.11	0.34 ± 0.05	22.6 ± 0.2
	800	32.4 ± 0.9	8.47 ± 0.95	0.29 ± 0.03	22.5 ± 0.1
LaNiAl	400	16.0 ± 0.3	10.1 ± 2.0	0.66 ± 0.15	23.3 ± 0.2
	450	15.6 ± 0.4	11.6 ± 2.7	0.76 ± 0.18	23.4 ± 0.2
	500	15.5 ± 0.3	11.5 ± 2.8	0.73 ± 0.20	23.4 ± 0.3
PdNiCuP	400	34.1 ± 1.0	8.80 ± 1.31	0.33 ± 0.09	22.6 ± 0.3
	800	30.5 ± 0.8	8.23 ± 0.65	0.28 ± 0.04	22.5 ± 0.1
MgCuGd	200	17.8 ± 2.8	4.27 ± 0.36	0.24 ± 0.02	22.3 ± 0.1
	400	15.6 ± 0.3	2.96 ± 0.15	0.19 ± 0.01	22.1 ± 0.1
	600	15.2 ± 0.8	2.58 ± 0.30	0.17 ± 0.02	21.9 ± 0.1
AuCuAgSi ($r = 2$ μm)	40	17.8 ± 3.2	11.0 ± 1.1	0.62 ± 0.06	23.2 ± 0.1
	60	19.7 ± 3.8	8.47 ± 0.40	0.43 ± 0.02	22.9 ± 0.1
	80	19.1 ± 4.8	7.45 ± 0.96	0.39 ± 0.05	22.8 ± 0.1

zones.[31–33] The five MGs exhibit distinct physical properties, for example, the yielding strength ranging from 0.5 GPa to 2 GPa and the glass transition temperature ranging from 420 K to 660 K.[34] Prior to indentations, the amorphous nature of the samples was confirmed by X-ray diffraction and differential scanning calorimetry; the sample surfaces were mechanically polished to a mirror finish. The nanoindentations were subsequently performed on the TI 950 TriboIndenter system[35] (Hysitron, Inc., Minneapolis, MN) with a 5 μm spherical indenter at room temperature (the Au-based alloy was performed with a 2–μm spherical indenter). Besides the ramping process, indentations were also held at loads, P_H, lower than 800 μN (as listed in Table I) to study the recovering effect. By virtue of the ultrafast data acquisition capability (with a maximum of ~30 000 points per second) of the nanoindentation system, high loading rates could be achieved. To reveal the effect of anelasticity, the loading time (t_L) was systematically varied from $\sim 10^0$ s to $\sim 10^{-4}$ s. In all of these tests, the holding time (t_H) and the unloading time (t_U) were fixed at 0.1 s, which sufficed to allow recovery of the anelastic deformation caused by the fast loading.

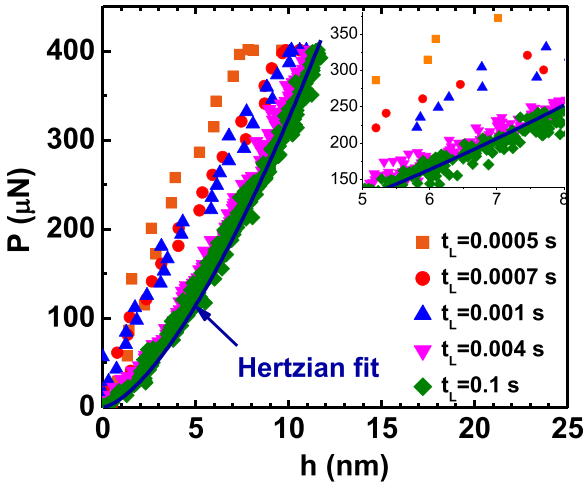

FIG. 1. Representative nanoindentation P–h curves for Pd-based MGs obtained at different loading rates. The fast loading curves (loading time t_L is small) exhibit anelastic characteristics that deviate from the Hertzian law, while the slow loading curves obey the Hertzian law. Inset: the magnified details to make the data more distinguishable.

III. RESULTS AND DISCUSSION

Figure 1 presents a series of nanoindentation load-displacement curves that are obtained with a maximum load of $P_H = 400$ μN. The Pd-based MG loading curves obey the Hertzian theory when loaded slowly, e.g., loading time t_L=0.004 s and 0.1 s. The loading curves deviate from the Hertzian theory when loaded fast, e.g., t_L=0.0005 s, 0.0007 and 0.001 s. This is consistent with the dynamic anelastic characteristics observed in other studies.[24,34,36]

Figure 2(a) shows a schematic core-shell structural model. The three-parameter model that is composed of two springs and a dash-pot is proposed to study the dynamic mechanical properties of the core-shell structure, as shown in Fig. 2(b). The loading depth is given as $h(t)^{3/2} = \frac{3P(t)(1-\upsilon)}{8\sqrt{r}G_I}$

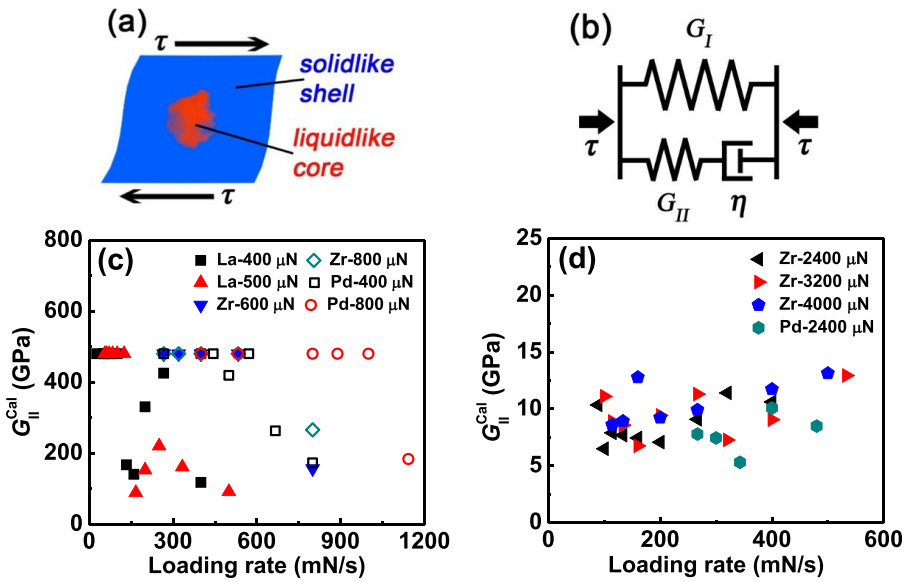

FIG. 2. (a) Sketch of the core-shell deformation unit in MGs. (b) Three-parameter viscoelastic model. (c) The calculated G_{II} in the three-parameter model *versus* the loading rate for low-load indentations of La-, Zr-, and Pd-based MGs. (d) The calculated G_{II} in the three-parameter model *versus* the loading rate indentations of Zr- and Pd-based MGs.

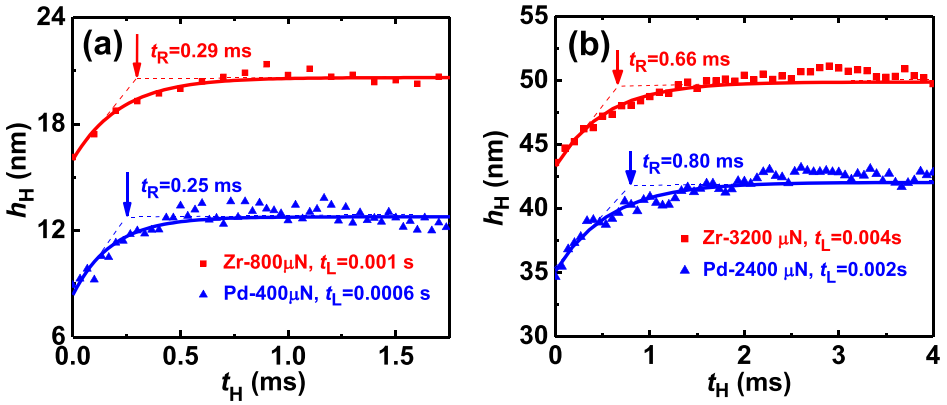

FIG. 3. The recovering process of indentation depth (h_H) *versus* the load-holding time (t_H). (a) The recovery process at low loads. The load is 800 μN and 400 μN for Zr-based (Vit 105) MG and Pd-based MGs, respectively. The ramping time is 0.001 s and 0.0006 s for Zr-based (Vit 105) MG and Pd-based MGs, respectively. (b) The recovery process at high loads. The load is 3200 μN and 2400 μN for Zr-based (Vit 105) MG and Pd-based MGs, respectively. The ramping time is 0.004 s and 0.002 s for Zr-based (Vit 105) MG and Pd-based MGs, respectively.

$-\frac{3\dot{P}(1-\upsilon)G_{II}t_c}{8\sqrt{r}(G_I+G_{II})}\left[1-\exp\left(-\frac{t}{t_c}\right)\right]$,[25,37] where G_I and G_{II} represent the shear modulus of parallel springs, η is the viscosity of the dashpot, r is the indenter tip radius, υ is Poisson's ratio, $\dot{P}$ is the loading rate, and t_c is the relaxation time. Figure 2(c) shows the G_{II} fitted by the three parameter model in different MGs. Its value is very large or even infinite beyond the normal range for the low load nanoindentations. But reasonable values can be achieved at a high load, as shown in Fig. 2(d). This suggests that the shear deformation process under a low load is different from that under a high load.

From another perspective, the anelastic deformation after the fast loading can be completely released after the load-holding process. Figures 3(a) and 3(b) show the recovery of anelastic deformation in different MGs *versus* the holding time at different loads. The recovery time (t_R) is between 0.3 ms at low loads and 0.8 ms at high loads, respectively. The discrepancy of t_R indicates a particular deformation behavior a under low load condition. Combined with the extremely large G_{II} and the shorter recovery time, the three-parameter model indeed degenerates to the Kelvin model for low load nanoindentations. Figure 4(a) presents the diagram of the Kelvin model and can be defined as:[25] $h(t)^{3/2}=\frac{3P(t)(1-\upsilon)}{8\sqrt{r}G_k}-\frac{3\dot{P}(1-\upsilon)t_c}{8\sqrt{r}(G_k)}\left[1-\exp\left(-\frac{t}{t_c}\right)\right]$, where G_k denotes the shear modulus of the spring, t_c is related to the activation energy ΔE through $t_c=\frac{\exp\left[\frac{\Delta E}{kT}\right]}{2\omega}$, ω is the debye frequency, k is the Boltzmann's constant, and T is the ambient temperature.[38]

For comparison between the three-parameter model and the Kelvin model, the fitting factor Δ is defined as $\Delta=\frac{S_{3p}-S_k}{N}$, $S=\sum_N\left(h_i^c-h_i^e\right)^2$, where h_i^c and h_i^e are the calculated and experimental nanoindentation depths, respectively, and N is the number of experimental data to be fitted in each curve. The parameter S indicates the fitting error of the models, i.e., S_{3p} is the fitting error of the 3-parameter model and S_k is the fitting error of the Kelvin model. Positive Δ indicates that the anelastic behavior fits the Kelvin model better compared to the 3-parameter model, and *vice versa*. As shown in Fig. 4(b), Δ is positive at low loads for three kinds of MGs. This denotes that the anelastic behavior of metallic glasses, at a low load, follows the Kelvin model.

Figure 5(a) shows the comparison of the experimental and theoretical loading-unloading curves at $P_H=500$ μN in La-based MGs. The unloading curve can be well fitted using the Hertzian theory, which indicates that the elastic deformation does not destroy the basic core-shell structure. The fast loading curve is well fitted by the Kelvin model. These fittings are also applicable for other MGs. The fitting parameters are listed in Table I. The calculated shear modulus G_k is close to the experimental data obtained in another work,[34] and t_c is similar to the recovery time in the load-holding process. Figure 5(b) shows the activation energy of the configurational transitions of liquid-like zones for different alloys which are almost the same, and $\Delta E=0.58$ eV$=23$ kT and are independent of the chemical components of MGs. Recently, Wang *et al.* discovered a fast β relaxation mode in addition to the slow β relaxation peak.[25] The activation energy of the fast β relaxation is about 0.53 eV, which is close to the value of liquid-like deformation. The activation energy at low load measured in this work is close to the fast β relaxation and much smaller than the slow β relaxation or

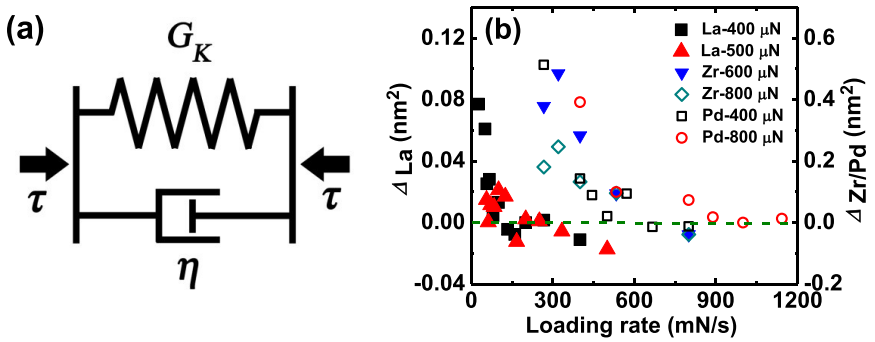

FIG. 4. (a) Sketch of the Kelvin viscoelastic model. (b) The calculated fitting factor Δ in Pd-based, La-based, and Vit105 MGs. Δ is positive at low loads which indicates that the anelastic behavior follows the Kelvin model.

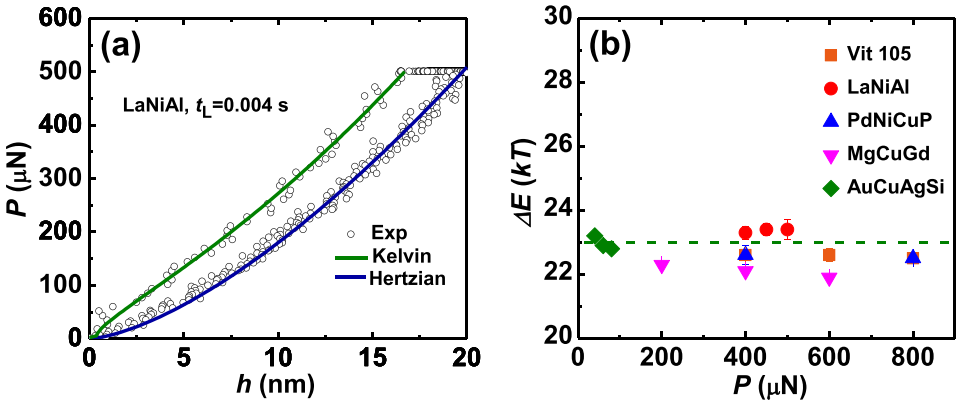

FIG. 5. (a) A representative loading-unloading curve for LaNiAl metallic glass. The loading curve can be well fitted using the Kelvin model (green curve), while the unloading curve can be well fitted using the Hertzian elastic contact theory (blue curve). (b) The activation energy (ΔE) of configurational transitions in liquid-like zones of different MGs, which is almost a constant and independent of the chemical compositions.

STZ ($\Delta E_\beta = 26RT_g$). As mentioned before, all the analyses and discussion should be based on the core-shell model. Slow β relaxation behavior is caused by the break of the elastic shell and the cooperative motion involving some core-shell units.[38] However, the fast β relaxation process derives from the excitation of loosely packaged atoms caged within their elastic surroundings. The chemical independent characteristic is probably related to the topological ordering transition for loose-packing zones. The structural origin of this new observed fast relaxation behavior needs further studies.

IV. CONCLUSIONS

In summary, we have studied the anelastic properties of MGs with different compositions and mechanical properties under low-load nanoindentation. The anelastic behaviors can be well fitted using the Kelvin model. The activation energy of configurational transitions encaged in the liquid-like zones is almost the same for 5 kinds of metallic glasses, about 0.58 eV, which is similar to the energy barriers of the fast β relaxation that were found in a La-based MG. The fast relaxation phenomenon may be attributed to the topological order transformation of liquid-like zones. These results provide a new insight in understanding the fundamental issues about relaxation and deformation in metallic glasses.

ACKNOWLEDGMENTS

The financial support from the National Natural Science Foundation of China (NSFC Nos. 11504931 and 51301188), the Zhejiang Provincial Natural Science Foundation of China (LY17E010005), the Instrument Developing Project of the Chinese Academy of Sciences (YZ201639), the One Thousand Talents Program of Zhejiang Province, and the One Hundred Talents Program of the Chinese Academy of Sciences is acknowledged.

[1]A. Inoue and A. Takeuchi, Acta Mater. **59**, 2243 (2011).
[2]A. Inoue, Acta Mater. **48**, 279 (2000).
[3]W. H. Wang, Adv. Mater. **21**, 4524 (2009).
[4]T. Egami, Rep. Prog. Phys. **47**, 1601 (1984).
[5]M. D. Ediger and P. Harrowell, J. Chem. Phys. **137**, 080901 (2012).
[6]J. Ding, S. Patinet, M. L. Falk, Y. Q. Cheng, and E. Ma, Proc. Natl. Acad. Sci. U. S. A. **111**, 14052 (2014).
[7]Y. Q. Cheng and E. Ma, Prog. Mater. Sci. **56**, 379 (2011).
[8]D. S. Gianola, Z. Lee, C. Ophus, E. J. Luber, D. Mitlin, U. Dahmen, K. J. Hemker, and V. R. Radmilović, Acta Mater. **61**, 1432 (2013).
[9]Y. Yang, J. F. Zeng, A. Volland, J. J. Blandin, S. Gravier, and C. T. Liu, Acta Mater. **60**, 5260 (2012).
[10]Y. H. Liu, D. Wang, K. Nakajima, W. Zhang, A. Hirata, T. Nishi, A. Inoue, and M. W. Chen, Phys. Rev. Lett. **106**, 125504 (2011).
[11]L. Liu, M. Hasan, and G. Kumar, Nanoscale **6**, 2027 (2014).
[12]C. Fan, P. K. Liaw, T. W. Wilson, W. Dmowski, H. Choo, C. T. Liu, J. W. Richardson, and T. Proffen, Appl. Phys. Lett. **89**, 111905 (2006).
[13]A. Hirata, P. Guan, T. Fujita, Y. Hirotsu, A. Inoue, A. R. Yavari, T. Sakurai, and M. Chen, Nat. Mater. **10**, 28 (2011).
[14]D. Ma, A. D. Stoica, and X. L. Wang, Nat. Mater. **8**, 30 (2009).
[15]K.-W. Park, J-i. Jang, M. Wakeda, Y. Shibutani, and J.-C. Lee, Scr. Mater. **57**, 805 (2007).
[16]J. Ding, Y. Q. Cheng, and E. Ma, Appl. Phys. Lett. **101**, 121907 (2012).
[17]H. L. Peng, M. Z. Li, and W. H. Wang, Phys. Rev. Lett. **106**, 135503 (2011).
[18]F. Zhu, H. K. Nguyen, S. X. Song, D. P. B. Aji, A. Hirata, H. Wang, K. Nakajima, and M. W. Chen, Nat. Commun. **7**, 11516 (2016).
[19]H. B. Ke, C. T. Liu, and Y. Yang, Science China-Technological Sciences **58**, 47 (2015).
[20]J. Schroers and W. L. Johnson, Phys. Rev. Lett. **93**, 255506 (2004).
[21]H. Kronmuller, J. Appl. Phys. **52**, 1859 (1981).
[22]W. H. Wang, Y. Yang, T. G. Nieh, and C. T. Liu, Intermetallics **67**, 81 (2015).
[23]R. D. Vaidyanathan, M. Ravichandran, G. Suresh, and S., Acta Mater. **49**, 3781 (2001).
[24]J. Q. Wang and J. H. Perepezko, J. Chem. Phys. **145**, 211803 (2016).
[25]Y. Yang, J. F. Zeng, J. C. Ye, and J. Lu, Appl. Phys. Lett. **97**, 261905 (2010).
[26]J. H. Perepezko, S. D. Imhoff, M. W. Chen, J. Q. Wang, and S. Gonzalez, Proc. Natl. Acad. Sci. U. S. A. **111**, 3938 (2014).
[27]K. Wang, D. Pan, M. W. Chen, W. Zhang, X. M. Wang, and A. Inoue, Mater. Trans. **47**, 1981 (2006).
[28]J. C. Ye, J. Lu, C. T. Liu, Q. Wang, and Y. Yang, Nat. Mater. **9**, 619 (2010).
[29]B. C. Wei, T. H. Zhang, W. H. Li, D. M. Xing, L. C. Zhang, and Y. R. Wang, Mater. Trans. **46**, 2959 (2005).
[30]L. S. Huo, J. F. Zeng, W. H. Wang, C. T. Liu, and Y. Yang, Acta Mater. **61**, 4329 (2013).
[31]T. P. Ge, W. H. Wang, and H. Y. Bai, J. Appl. Phys. **119**, 204905 (2016).
[32]Z. Wang, B. A. Sun, H. Y. Bai, and W. H. Wang, Nat. Commun. **5**, 5823 (2014).
[33]H. B. Ke, J. F. Zeng, C. T. Liu, and Y. Yang, J. Mech. Sci. Technol. **30**, 560 (2014).
[34]W. H. Wang, Prog. Mater. Sci. **57**, 487 (2012).
[35]See https://www.hysitron.com/products-services/standalone-instruments/ti-950-triboindenter for the details of experimental setup.
[36]C. A. Schuh, Mater. Today **9**, 32 (2006).
[37]L. S. Huo, J. Ma, H. B. Ke, H. Y. Bai, D. Q. Zhao, and W. H. Wang, J. Appl. Phys. **111**, 113522 (2012).
[38]Y. Wang, M. Liu, L. L. Wang, G. Q. Li, L. N. Dong, and D. Z. Sun, J. Mol. Liquids **169**, 15 (2012).